

## **Supplementary material for**

### **Stem-loop binding protein is a multifaceted cellular regulator of HIV-1**

Ming Li, Lynne T. Tucker, John M. Asara, Collins K. Cheruiyot, Huafei Lu, Zhijin J. Wu, Michael C. Newstein, Mark S. Dooner, Jennifer Friedman, Michelle A. Lally, Bharat Ramratnam

The main PDF includes the following:

Supplementary Materials and Methods

Supplementary Texts

Supplementary Figures 1 to 17

Supplementary References

Supplementary Tables 1 to 12 are attached separately.

## **SUPPLEMENTARY MATERIALS AND METHODS:**

**1. Viability assays:** MTT assay (MilliporeSigma) was used to measure cellular proliferation after siRNA transfection. All procedures were performed according to the manufacturer's instruction.

**2. Establishment of stable CEM cell lines with depleted SLBP:** SMARTvector™ 2.0 lentiviral shRNA particles against SLBP and non-target control (GE Dharmacon) were used to transduce CEM cells by following the manufacturer's instructions. Briefly, cells were cultured in CEM medium (RPMI-1640+10% FBS) without puromycin for 48h after transduction. The transduced cells were then transferred into CEM medium containing 0.3 µg/mL puromycin and subjected to further expansion. Medium was replaced every 2-3 days and cells were passaged as needed for four weeks. A fraction of surviving cells was then harvested to check knockdown efficiency. After verification, the SLBP depleted cells were maintained in CEM medium and used to perform various downstream assays.

**3. Flow Cytometry:** To assess receptor and co-receptor levels, Hela-T4 cells, transfected by non-target control and SLBP siRNAs, were harvested at 48h post-transfection. Cells were washed and re-suspended in ice cold FACS Analysis Buffer (sterile filtered PBS + 0.5% FBS + 0.2% Azide), then stained with the following antibodies: mouse anti-Human CD4, conjugated with APC (BD Biosciences, San Jose, CA), mouse anti-Human CXCR4, conjugated with PE (BD Biosciences). After staining, cells were washed twice with FACS buffer and analyzed using an LSRII flow cytometer (BD Biosciences).

**4. Formaldehyde Assisted Isolation of Regulatory Elements (FAIRE) assay:** FAIRE assay was performed according to procedures described by Giresi et al (1). Briefly, chromatin was cross-linked with formaldehyde, sheared by sonication, and phenol-chloroform extracted. The

amount of DNA recovered in the aqueous phase (euchromatin) was then quantified by Quant-iT™ DNA Assay Kit (high sensitivity) on Qubit® 2.0 Fluorometer (Thermo Fisher Scientific). Finally, the amount of euchromatin DNA was compared between the control and SLBP depleted cells. Genomic DNA was also isolated and quantified to standardize the input for FAIRE assay.

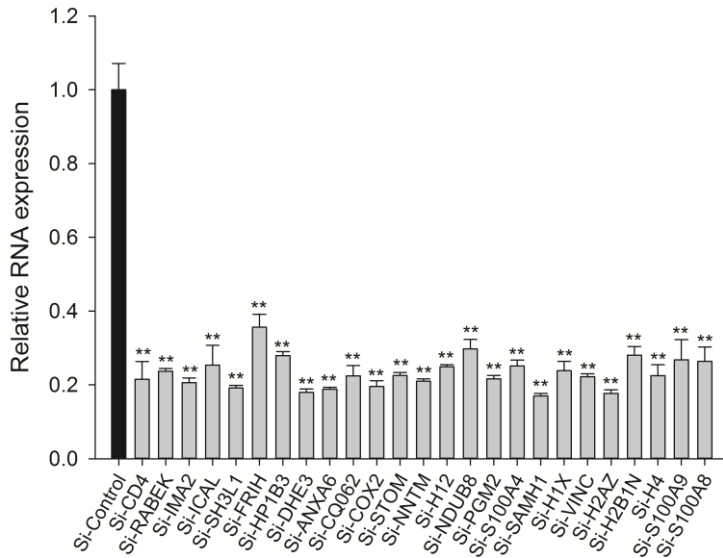
#### **SUPPLEMENTARY TEXT:**

**SLBP depletion on viral life cycle: a) Binding:** To determine whether SLBP depletion had any effect on cell surface receptors for HIV-1, we analyzed the CD4 and CXCR4 levels on HeLa-T4 cells by FACS. We did not observe significant differences in either CD4 or CXCR4 levels between SLBP depleted cells and matched controls at 48h post-transfection (Supplementary Figure 11).

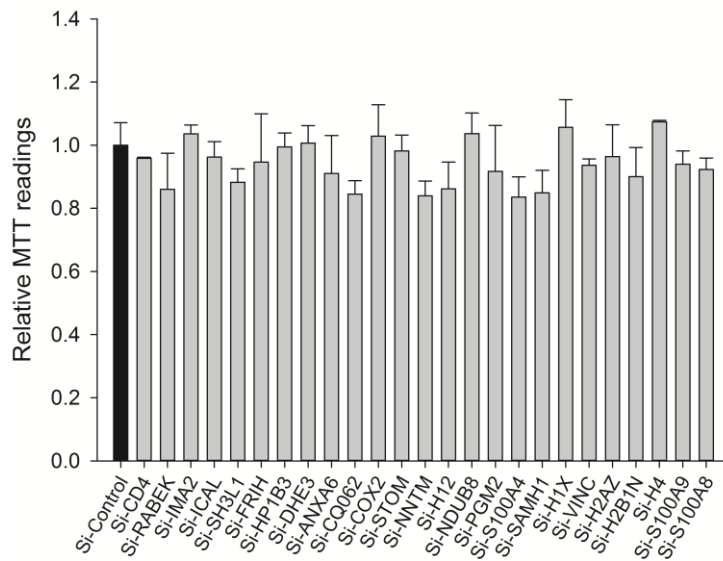
**b) Reverse transcription:** We also compared the levels of early reverse transcription (ERT) and late reverse transcription (LRT) products between SLBP depleted cells and matched controls at 48h post-infection. No significant difference was observed for both ERT and LRT levels (Supplementary Figure 12).

**c) Budding:** We examined the possible effects of SLBP depletion on HIV-1 budding by surveying the expression of four critical host proteins, ALIX (ALG-2-interacting protein X) (2), BST2 (bone marrow stromal antigen 2, also known as Tetherin) (3, 4), TSG101 (Tumor susceptibility gene 101) (5) and VPS4 (Vacuolar protein sorting-associated protein 4) (6), responsible for viral budding (7). We found that SLBP depletion had no impact on the expression levels of any of these proteins (Supplementary Figure 13).

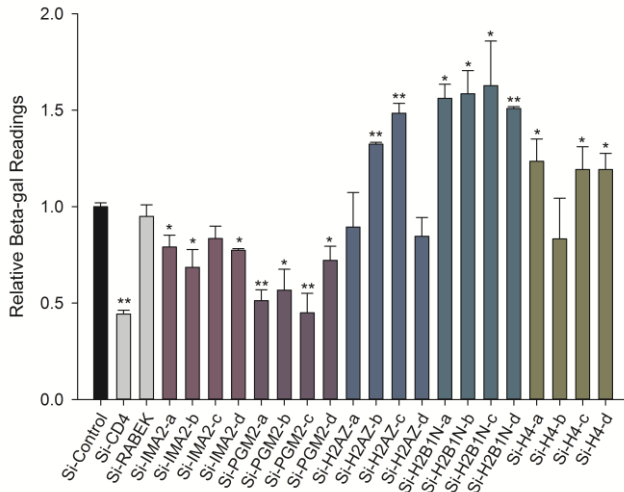
**SUPPLEMENTARY FIGURES:**



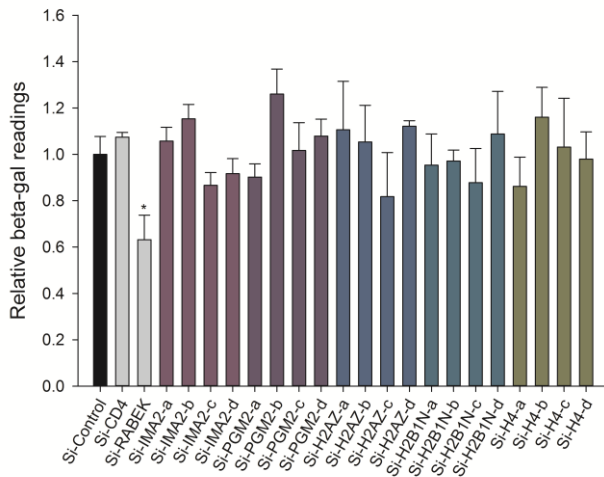
**Supplementary Figure 1.** The siRNA knockdown efficiency of the twenty-three candidates and the two positive controls. TZM-bl cells were transfected with SMARTpool siRNAs against each gene. 24h post-transfection, RNAs were extracted and subjected to RT-PCR quantification. RNA expression of each gene was compared to the control sample transfected with non-target siRNAs. (n = 3 biological replicates). Student's *t*-test; \*\*,  $p < 0.01$ ; Error bars represent  $\pm$ SD.



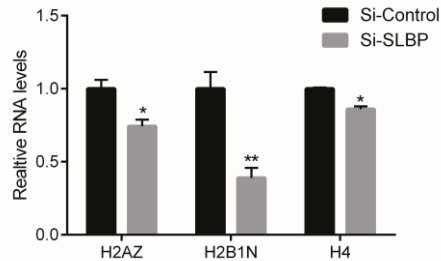
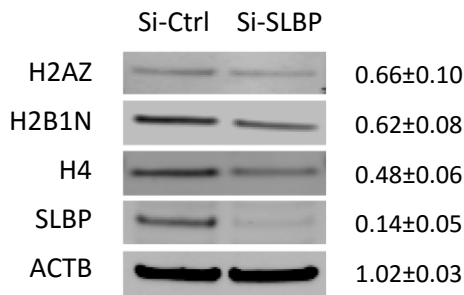
**Supplementary Figure 2.** Cell proliferation rates under siRNA depletion. TZM-bl cells were transfected with SMARTpool siRNAs against each candidate gene. 24h post-transfection, MTT-based assays were employed to analyze the effect of siRNA depletion on cell proliferation. Compared to the control sample transfected with non-target siRNAs, no significant changes of proliferation rates were observed. (n = 3 biological replicates). Student's *t*-test; Error bars represent  $\pm$ SD.



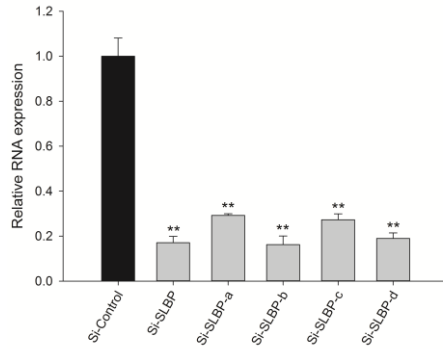
**Supplementary Figure 3. Phase I  $\beta$ -gal assay results of the individual siRNA against the 5 hits.** siRNA transfected and HIV-1 infected TZM-bl cells were lysed, exposed to a  $\beta$ -gal substrate, and relative  $\beta$ -gal readings were recorded. Non-target siRNA control (negative control), siRNAs against CD4 (positive control for Phase I) and RABEK (positive control for Phase II) were also employed. (n = 3 biological replicates). Student's *t*-test; \*\*,  $p < 0.01$ ; \*,  $p < 0.05$ ; Error bars represent  $\pm$ SD.



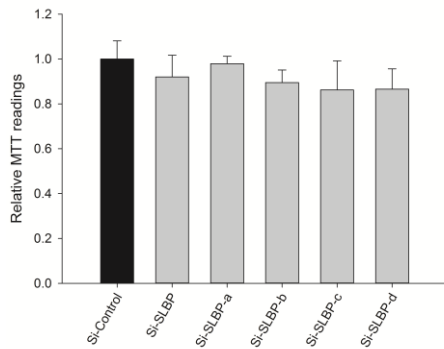
**Supplementary Figure 4. Phase II  $\beta$ -gal assay results of the individual siRNA against the 5 hits.** The fresh cells, treated with culture supernatant (p24 adjusted) from Phase I, were lysed, exposed to a  $\beta$ -gal substrate, and relative  $\beta$ -gal readings were recorded. Non-target siRNA controls (negative control), siRNA against CD4 (positive control for Phase I) and RABEK (positive control for Phase II) were also employed. (n = 3 biological replicates). Student's *t*-test; \*,  $p < 0.05$ ; Error bars represent  $\pm$ SD.



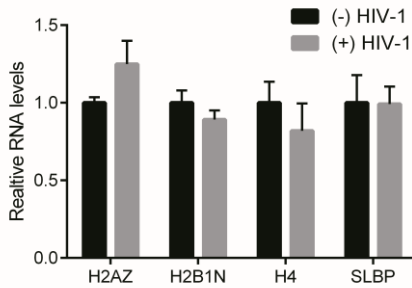
**Supplementary Figure 5. Cellular SLBP depletion reduces the expression of histone candidates at protein (left panel) and mRNA (right panel) level.** Protein and RNA were extracted from Hela-T4 cells at 48h post-transfection. The relative expression of three histones (H2AZ, H2B1N and H4) was shown by western blotting (left panel) and real-time PCR (right panel). Comparison was conducted between cells transfected with non-target siRNAs and those transfected with SLBP siRNAs. (n = 3 biological replicates). Student's *t*-test; \*\*,  $p < 0.01$ ; \*,  $p < 0.05$ ; Error bars represent  $\pm$ SD.



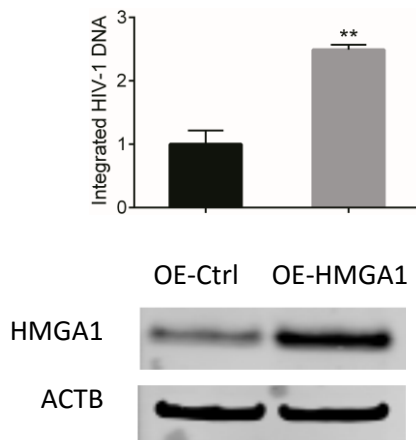
**Supplementary Figure 6. Gene knockdown efficiency of individual siRNA targeting SLBP.** TZM-bl cells were transfected with SMARTpool siRNAs against SLBP (“SLBP”) and the four individual SLBP siRNA (“SLBP a-d”). 24h post-transfection, RNA was extracted and subjected to RT-PCR quantification. RNA expression was compared between each SLBP siRNA treated sample and control sample transfected with non-target siRNAs. (n = 3 biological replicates). Student’s *t*-test; \*\*,  $p < 0.01$ ; Error bars represent  $\pm$ SD.



**Supplementary Figure 7. Cell proliferation rates under SLBP siRNA depletion.** TZM-bl cells were transfected with SLBP SMARTpool siRNAs (“SLBP”) and four individual siRNA (“SLBP a-d”). 24h post-transfection, MTT-based assays were employed to analyze the effect of siRNA depletion on cell proliferation rates. Compared to the control cells transfected with non-target siRNAs, no significant changes of proliferation rates were observed. (n = 3 biological replicates). Student’s *t*-test; Error bars represent  $\pm$ SD.



**Supplementary Figure 8. HIV-1 infection itself did not significantly affect the expression of the histone candidates and SLBP.** The relative mRNA expression of the three histones (H2AZ, H2B1N and H4) and SLBP were examined by real-time PCR in HIV-1 infected/uninfected PBMCs. (n = 3 biological replicates). Student’s *t*-test; Error bars represent  $\pm$ SD.

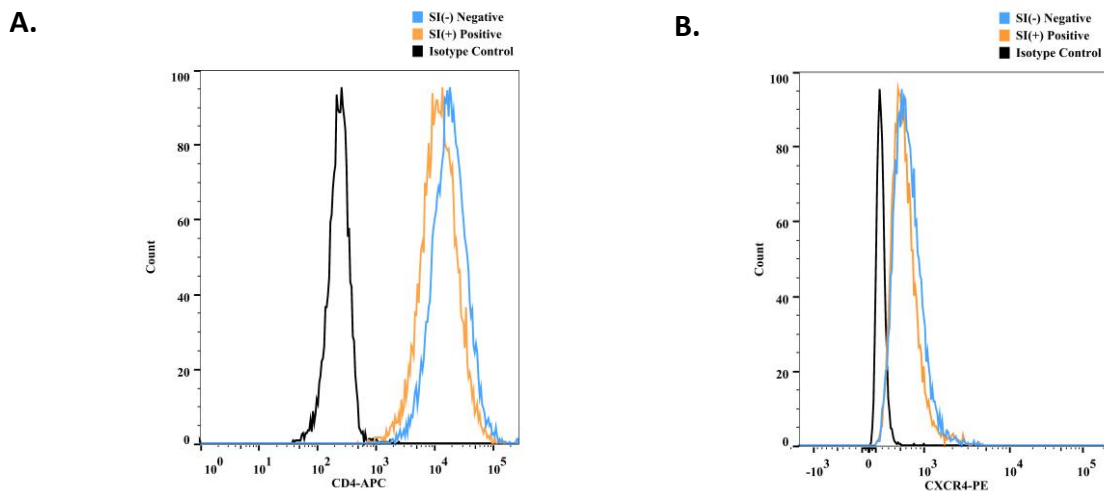


**Supplementary Figure 9. Over-expressed HMGA1 was associated with significantly higher HIV-1 integration levels.** Vectors bearing HMGA1 over-expressing cassette (OriGene; Catalog, SC319124) and control plasmid (OriGene; Catalog, PS100020) were transfected into Hela-T4 cells. 24h after transfection, cells were infected by HIV-1<sub>NL4-3</sub> for 48h. DNA was then extracted, and Alu PCR was used to quantify HIV-1 integration levels. HMGA1 overexpression was verified by western blot. ACTB was used as the loading control. (n = 3 biological replicates). Student’s *t*-test; \*\*,  $p < 0.01$ ; Error bars represent  $\pm$ SD.

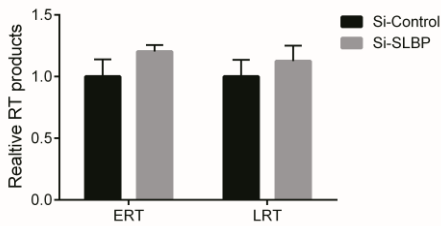
5'-

ATGGCCTGCCGCCCGGAAGCCCGCCGAGGCATCAGAGCCGCTGCGACGGTGACGCCAGCCCGCCGTCCCCGCGGATGGA  
GCCTGGGACGGAAGCGCAGAGCCGACGGCAGGCGCTGGAGGCCGAAGACGCCGAGGAGGCAGAGCACCGCGGCCGA  
GCGCAGACCCGAGAGCTTTACCACTCCTGAAGGCCCTAAACCCGTTCCAGATGCTCTGACTGGGCAAGTGCAGTTGAAGAAG  
ATGAGATGAGAAACAAGGGTGAACAAAGAAATGGCAAGATATAAAAGGAAACTCCTCATCAATGACTTTGGAAGAGAGAGAA  
AATCATCATCAGGAAGTTCTGATTCAAAGGAGTCTATGTCTACTGTGCCGCCGATTTGAAACCGATGAAAGTGTCTAATGA  
GGAGGCAAAAACAATTAATTATGGGAAGAACAATTGCCTACGATCGTTATATTAAGAAGTCCAAGACACCTTCGACAA  
CCTGGCATTTCATCCAAGACCCCTAATAAATTTAAAAATACAGCCGGCGCTCTGGGACCAGCAAATCAAATCTGGAAGGT  
GGCTCTGCATTTTTGGGATCCTCCAGCGGAAGAAGGATGTGATTTGCAAGAAATACACCCTGTAGACCTTGAATCTGCAGAAA  
GCAGCTCCGAGCCCCAGACCAGCTCTCAGGATGACTTTGATGTGTACTCTGGCACACCCACCAAGGTGAGACACATGGACAGT  
CAAGTGGAGGATGAGTTTGATTGGAAGCTTGTTAACTGAACCCTTGAGAGACTTCTCAGCCATGAGCTAG-3'

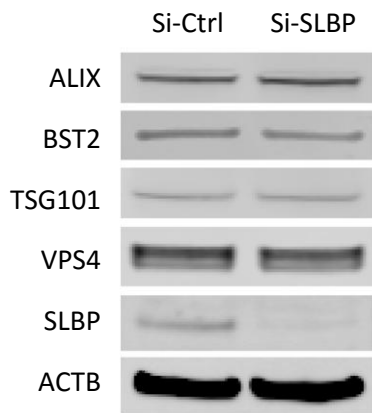
**Supplementary Figure 10. The synthesized cDNA sequence of SLBP that is resistant to SMARTpool SLBP siRNA degradation.** The four siRNA targeted fragments (yellow highlight) were subjected to mutations. The mutated nucleotides are shown in red color. The synthesized SLBP encodes the same amino acid sequence as wide-type SLBP.



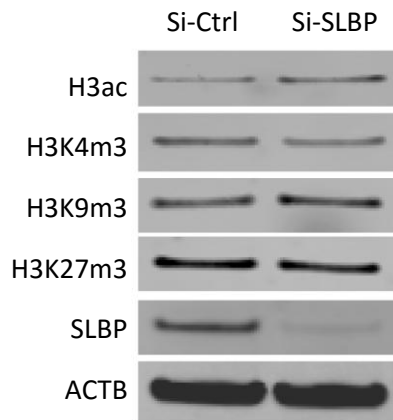
**Supplementary Figure 11. The expression of HIV-1 receptor and co-receptor on host cells when SLBP was depleted.** **A).** SLBP depletion was not associated with significant changes in surface CD4 levels on host cells. HeLa-T4 cells, transfected with the siRNAs against SLBP (Yellow line) or non-target siRNA controls (Blue line), were stained with anti-CD4-APC at 48h post-transfection and analyzed by FACS. Isotype match-APC control (black line). **B).** SLBP depletion was not associated with significant changes in CXCR4 levels on host cells. HeLa-T4 cells, transfected with the siRNAs against SLBP (Red line) or non-target siRNA controls (Blue line), were stained with anti-CXCR4-PE, at 48h post-transfection and analyzed by FACS. Isotype match-PE control (black line). (n = 3 biological replicates).



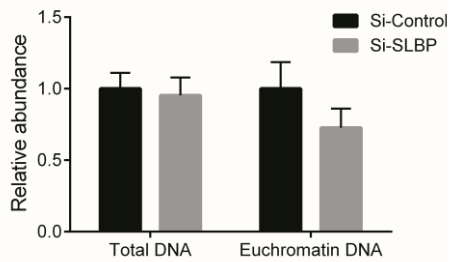
**Supplementary Figure 12. The expression of HIV-1 reverses transcription products when SLBP was depleted.** SLBP depletion did not affect levels of early reverse transcriptase products (ERT) and late transcript products (LRT) at 48h post-infection in HIV-1 infected HeLa-T4 cells. (n = 3 biological replicates). Student's *t*-test; Error bars represent  $\pm$ SD.



**Supplementary Figure 13. SLBP depletion had no appreciable effect on critical host factors involving in viral budding.** HeLa-T4 cells were transfected by non-target control and SLBP siRNAs. 48h after transfection, total proteins were extracted, and western blotting was used to examine protein expression of ALIX, BST2, TSG101 and VPS4. ACTB was used as the loading control. (n = 3 biological replicates).

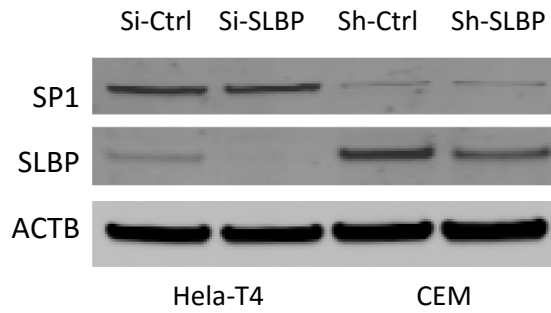


**Supplementary Figure 14. The profiling of representative histone markers showed that SLBP depletion had no significant effect on post-translational modifications.** Total protein was extracted from transfected HeLa-T4 cells at 48h post-transfection. The expression of two activational (H3ac and H3K4m3, commonly found in euchromatin) and two repressive (H3K9m3 and H3K27m3, commonly found in heterochromatin) histone marks were examined by western blotting. Beta-actin (ACTB) was used as a loading control. (n = 3 biological replicates).

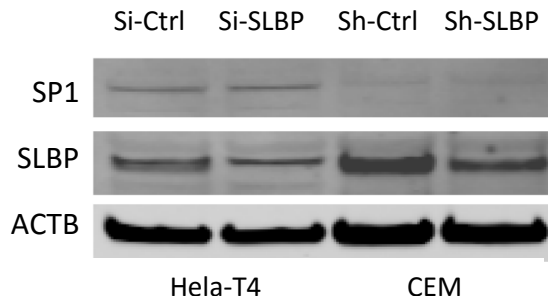


**Supplementary Figure 15. SLBP depletion has no significant effect on the abundance of euchromatin.**

Hela-T4 cells were transfected by control and SLBP siRNAs. 48h after transfection, fractions containing abundant active regulatory elements (euchromatin) were isolated by FAIRE. The amount of euchromatin was quantified by a Qubit 2.0 fluorometer. The abundances of euchromatin were compared between the control and SLBP depleted cells. Total genomic DNAs were used as the input control. (n = 3 biological replicates). Student's *t*-test; Error bars represent  $\pm$ SD.



**Supplementary Figure 16. SLBP depletion has no appreciable effect on SP1 expression.** Total proteins were extracted from HeLa-T4 cells (transiently transfected by SLBP siRNAs) and CEM cells (stably expressing SLBP shRNA). Western blotting was employed to examine SP1 expression. ACTB was used as the loading control. (n = 3 biological replicates).



**Supplementary Figure 17. In HIV-1 infected cells, SLBP depletion also had no appreciable effect on SP1 expression.** HeLa-T4 cells (transiently transfected by SLBP siRNAs) and CEM cells (stably expressing SLBP shRNA) were infected with HIV-1<sub>NL4-3</sub>. At 48h post-infection, total proteins were extracted. Western blotting was employed to examine SP1 expression. ACTB was used as the loading control. (n = 3 biological replicates).

## **SUPPLEMENTARY TABLES**

**Supplementary Table 1.** CD4 count and plasma viral load of the twenty study subjects employed in initial proteomic screen.

**Supplementary Table 2.** Original mass spectrometry data from the two independent proteomic screens.

**Supplementary Table 3.** Detailed calculation of cutoff values for protein perturbation.

**Supplementary Table 4.** Detailed information of the initial fifty-five candidates from Group 1 and the seventy-four candidates from Group 2.

**Supplementary Table 5.** The twenty-three shared candidates between the two independent proteomic screens. Protein name, uniprot database access, molecular weight and SILAC ratios from Group 1 and 2 are given. The established interactions with HIV-1 encoded proteins are also shown.

**Supplementary Table 6.** Detailed DAVID analysis of the twenty-three candidates from the proteomic screens.

**Supplementary Table 7.** In vivo and in vitro RNA and protein quantification revealed a similar expression pattern between the three histones (H2AZ, H2B1N and H4) and SLBP.

**Supplementary Table 8.** Small interfering RNAs employed in this study. Their names, corresponding genes, catalog numbers and nucleotide sequences are given.

**Supplementary Table 9.** PCR primers employed in this study. Their names and sequences are given.

**Supplementary Table 10.** Antibodies employed in this study. Their names, catalog numbers and vendors are given.

**Supplementary Table 11.** CD4 count and plasma viral load of the twenty-seven study subjects employed in Figure 6C of individual TNF $\alpha$  quantification.

**Supplementary Table 12.** CD4 count and plasma viral load of the ninety study subjects employed in Figure 6D of individual SLBP quantification.

#### **SUPPLEMENTARY REFERENCE**

1. Giresi PG, and Lieb JD. Isolation of active regulatory elements from eukaryotic chromatin using FAIRE (Formaldehyde Assisted Isolation of Regulatory Elements). *Methods*. 2009;48(3):233-9.
2. Strack B, Calistri A, Craig S, Popova E, and Gottlinger HG. AIP1/ALIX is a binding partner for HIV-1 p6 and EIAV p9 functioning in virus budding. *Cell*. 2003;114(6):689-99.
3. Neil SJ, Zang T, and Bieniasz PD. Tetherin inhibits retrovirus release and is antagonized by HIV-1 Vpu. *Nature*. 2008;451(7177):425-30.
4. Mangeat B, Gers-Huber G, Lehmann M, Zufferey M, Luban J, and Piguet V. HIV-1 Vpu neutralizes the antiviral factor Tetherin/BST-2 by binding it and directing its beta-TrCP2-dependent degradation. *PLoS Pathog*. 2009;5(9):e1000574.
5. Garrus JE, von Schwedler UK, Pornillos OW, Morham SG, Zavitz KH, Wang HE, Wettstein DA, Stray KM, Cote M, Rich RL, et al. Tsg101 and the vacuolar protein sorting pathway are essential for HIV-1 budding. *Cell*. 2001;107(1):55-65.
6. Stuchell-Brereton MD, Skalicky JJ, Kieffer C, Karren MA, Ghaffarian S, and Sundquist WI. ESCRT-III recognition by VPS4 ATPases. *Nature*. 2007;449(7163):740-4.
7. Sundquist WI, and Krausslich HG. HIV-1 assembly, budding, and maturation. *Cold Spring Harb Perspect Med*. 2012;2(7):a006924.